

Dispersion relation of guided-mode resonances and Bragg peaks in dielectric diffraction gratings

Sara Nilsen-Hofseth and Víctor Romero-Rochín*

Instituto de Física, Universidad Nacional Autónoma de México, Apartado Postal 20-364, 01000 México, Distrito Federal, Mexico

(Received 8 March 2001; published 29 August 2001)

We present the dispersion relation of guided-mode resonances in non-dissipative dielectric diffraction gratings, both for s -polarized (TE mode) and p -polarized (TM mode) incident waves. We present a simple approximate theory as well as a rigorous calculation within the so-called coupled-wave theory. We discuss the dependence of the positions and the lifetimes of the resonances on the thickness of the gratings and on the strength of its modulation. We find that the diffraction efficiency of the different orders show peaks at different Bragg orders.

DOI: 10.1103/PhysRevE.64.036614

PACS number(s): 42.25.Fx, 42.25.Bs

I. INTRODUCTION

Simple diffraction gratings offer a very rich variety of optical phenomena not only from a fundamental point of view but also from their enormous potential for applications. In particular, modulated dielectric diffraction gratings have been a focus of attention for some time. Modulated diffraction gratings give rise to such interesting phenomena as guided-mode resonances [1–4], Bragg diffraction [5–7], diffraction of pulses [8–10], and diffraction through heterostructures [11–15]. Among the most widely implemented applications is the design of gratings as optical filters [16–27]. A motivation for our study is the understanding of the diffraction of ultrashort light pulses by spatiotemporal gratings [28,29].

The theoretical understanding of the diffraction through modulated gratings is, in principle, given by the so-called coupled-wave theory introduced by Moharam and Gaylord [30–33], which is an ansatz solution of Maxwell equations for this class of problems. Nonetheless, such a solution has not been found in an analytical closed form, and the problem is so rich that there are still many questions to be resolved.

The purpose of this article is to provide a concise summary of the diffraction of an electromagnetic wave through a sinusoidally modulated grating by means of dispersion relations of the guided-mode resonances [1–4]. From the corresponding graphical representations of the dispersion relations one can obtain a clear physical picture of the behavior of the diffraction efficiencies, as functions of frequency and angle of incidence, information on the material eigenmodes and diffraction orders, the positions of guided-mode resonances, and the appearance of Bragg peaks.

We proceed by presenting results from an exact numerical analysis of the coupled-wave theory and from simple approximate theoretical arguments. We treat both TE and TM modes (i.e., electric field polarization perpendicular or parallel to the plane of incidence). Section II presents a quick review of the coupled-wave theory. We emphasize the fact that the coupled-wave equations give rise to material eigenmodes that can be classified according to their dependence

on the electromagnetic and grating wave vectors and in their propagating or evanescent character. This yields a clear physical picture of the origin of the guided-mode resonances. In our opinion, these aspects have not yet been thoroughly analyzed in the current literature. Section III is the main contribution of this article and is devoted to the dispersion relations of the waveguide resonances for both types of polarizations. In that section we also make a brief description of the dependence of the resonances on the dielectric grating modulation and on the geometric thickness of the grating. Next, in Sec. IV, we show the appearance of the Bragg peaks and point out that higher diffraction orders have peaks at higher order Bragg angles; this has not been appreciated previously. We provide a nonrigorous explanation for this interesting and potentially useful phenomenon. We conclude this paper in Sec. V.

II. COUPLED-WAVE THEORY AND DIFFRACTION EFFICIENCIES

The simplest way to pose the problem is to consider a dielectric slab in vacuum, infinite in the x - z plane and of thickness d in the y direction. The diffraction grating is described by a dielectric function spatially modulated in the x direction, namely,

$$\epsilon(x) = \epsilon_0 + \epsilon_1 \cos(Kx), \quad (1)$$

where ϵ_0 is the average background dielectric constant and ϵ_1 is the strength of the modulation. This is the problem as originally considered by Born and Wolf [34], where diffraction of light by ultrasonic waves is studied. One can consider more complicated dielectric gratings, with several different periodic functions, or placed between different dielectric media, or with a slanted wavevector K dependence [33]. These may be needed in order to describe a particular experimental situation, but as we shall see, the qualitative phenomenon is clearly independent of those details. Although ϵ_0 and ϵ_1 may have arbitrary values, waveguide resonances can be easily explained if one considers $\epsilon_0 \gg \epsilon_1$. We shall later on describe the differences when these dielectric constants are of the same order of magnitude.

An s - or p -polarized em wave of frequency ω is incident on the grating at an angle θ with the y direction, and the

*Corresponding author. FAX: (52) 5622 5015. Email address: romero@fisica.unam.mx

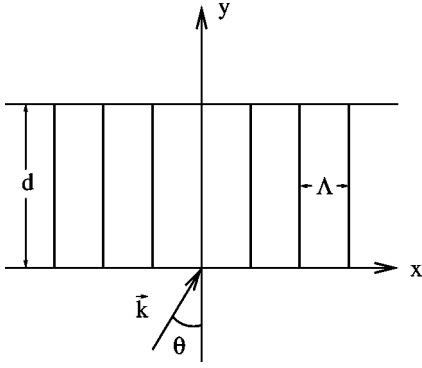


FIG. 1. The system setup. The system is infinite in the z direction. The dielectric function is given by $\epsilon(x) = \epsilon_0 + \epsilon_1 \cos(Kx)$, with $K = 2\pi/\Lambda$.

problem consists in finding the fields inside the grating as well as the reflected and transmitted ones; see Fig. 1. We shall call TE the case of s -polarized waves and TM the case of p -polarized waves since in the former the fields inside the grating are similar to TE modes and in the latter to TM modes in a waveguide. The incident TE electric field is

$$\vec{E}_{inc}(x, y, t) = \hat{z} E_0 e^{i\vec{k} \cdot \vec{r}} e^{-i\omega t} \quad (\text{TE}) \quad (2)$$

and the incident TM magnetic field is

$$\vec{B}_{inc}(x, y, t) = \hat{z} B_0 e^{i\vec{k} \cdot \vec{r}} e^{-i\omega t}, \quad (\text{TM}) \quad (3)$$

where the incident wave vector is given by $\vec{k} = (k_x, k_y)$ with $k_x = k \sin \theta$. The ensuing reflected and transmitted fields are expressed as

$$\vec{E}_{out}^{\pm}(x, y, t) = \hat{z} \sum_l A_l^{\pm} e^{\pm i k_{ly} y} e^{i(k_x + lK)x} e^{-i\omega t} \quad (\text{TE}) \quad (4)$$

and

$$\vec{B}_{out}^{\pm}(x, y, t) = \hat{z} \sum_l C_l^{\pm} e^{\pm i k_{ly} y} e^{i(k_x + lK)x} e^{-i\omega t} \quad (\text{TM}) \quad (5)$$

where the superindex (+) refers to $y \geq d$ (transmitted) and (-) to $y \leq 0$ (reflected). The wave vector component k_{ly} is given by ($c \equiv 1$, so that $k = \omega$)

$$k_{ly} = \sqrt{\omega^2 - (k_x + lK)^2}. \quad (6)$$

The different values of l of the field outside the grating are called the *diffraction orders*, which can be either propagating or evanescent depending on whether the component k_{ly} is real or imaginary. The amplitudes A_l^{\pm} and C_l^{\pm} are found by matching boundary values with the fields inside the grating.

The solutions inside the gratings follow from applying Maxwell equations to the ansatz known as coupled-wave theory [30–33]. That is, the fields inside are assumed to be a sum of coupled waves,

$$\vec{E}_{in}(x, y, t) = \hat{z} \sum_l V_l(y) e^{i(k_x + lK)x} e^{-i\omega t} \quad (\text{TE}) \quad (7)$$

and

$$\vec{B}_{in}(x, y, t) = \hat{z} \sum_l U_l(y) e^{i(k_x + lK)x} e^{-i\omega t} \quad (\text{TM}) \quad (8)$$

with $l = \dots, -1, 0, 1, \dots$. Due to the x dependence of the dielectric function $\epsilon(x)$, the amplitudes $V_l(x)$ and $U_l(x)$ are coupled for all values of l through the set of equations (that follow from direct application of Maxwell equations),

$$\begin{aligned} \frac{d^2 V_l(y)}{dy^2} + [\epsilon_0 \omega^2 - (k_x + lK)^2] V_l(y) \\ + \frac{1}{2} \epsilon_1 \omega^2 [V_{l-1}(y) + V_{l+1}(y)] = 0 \quad (\text{TE}) \quad (9) \end{aligned}$$

and

$$\begin{aligned} \epsilon_0 \frac{d^2 U_l(y)}{dy^2} + \frac{1}{2} \epsilon_1 \frac{d^2 U_{l-1}(y)}{dy^2} + \frac{1}{2} \epsilon_1 \frac{d^2 U_{l+1}(y)}{dy^2} \\ + \left[\left(\epsilon_0 + \frac{\epsilon_1^2}{2\epsilon_0} \right) \omega^2 - (k_x + lK)^2 \right] \epsilon_0 U_l(y) \\ + \left[\epsilon_1 \epsilon_0 \omega^2 + \frac{1}{2} \epsilon_1 \omega (k_x + (l-1)K) \right. \\ \left. - \frac{1}{2} \epsilon_1 [k_x + (l-1)K]^2 \right] \\ \times U_{l-1}(y) + \left(\epsilon_1 \epsilon_0 \omega^2 - \frac{1}{2} \epsilon_1 \omega [k_x + (l+1)K] \right. \\ \left. - \frac{1}{2} \epsilon_1 [k_x + (l+1)K]^2 \right) U_{l+1}(y) \\ + \frac{1}{4} \epsilon_1^2 \omega^2 U_{l-2}(y) + \frac{1}{4} \epsilon_1^2 \omega^2 U_{l+2}(y) = 0 \quad (\text{TM}). \quad (10) \end{aligned}$$

These sets of equations can be cast into eigenvalue problems in which the matrices to be diagonalized are orthogonal with real elements. Hence, the corresponding eigenvalues, denoted as $\kappa_n^2 = \kappa_n^2(K, \omega, k_x)$, are real but they can be either positive or negative [35]. The functions $V_l(y)$ and $U_l(y)$ can therefore be expressed as (infinite) sums of eigenmodes of the material, namely,

$$V_l(y) = \sum_n [A_n a_{nl} e^{i\kappa_n y} + B_n a_{nl} e^{-i\kappa_n y}], \quad (11)$$

and with an analogous expression for $U_l(y)$. The eigenmodes a_{nl} correspond to the eigenvalues κ_n^2 of the above-mentioned matrix. We note that the solutions $V_l(y)$ and $U_l(y)$ are expressed in terms of the wave vectors κ_n that are the square roots of the eigenvalues. Therefore, the wave vectors κ_n are purely real or purely imaginary; they have a very

important physical meaning and, accordingly, we shall call them propagating or evanescent *eigenmodes* of the material, depending on whether they are real or imaginary. One must keep in mind that these are electromagnetic eigenmodes of a material with a dielectric function given by $\epsilon(x)$, Eq. (1); that is, they are independent of the thickness d of the grating. Clearly, if $\epsilon_1 \ll \epsilon_0$, from Eqs. (9) and (10) one finds that the eigenmodes are approximately given by

$$\kappa_n \approx [\omega^2 \epsilon_0 - (k_x + nK)^2]^{1/2}. \quad (12)$$

As we shall see in Sec. III, the guided-mode resonances appear when the number of propagating eigenmodes is larger than the number of propagating diffraction orders.

The measurable quantities to be calculated are the reflected and transmitted diffraction efficiencies [33]. These are defined as the ratio of the y components of the reflected or transmitted Poynting vectors to the incident one, averaged over one grating wave length $2\pi/K$ in the x direction and over one period $2\pi/\omega$. These efficiencies are a measure of the energy transmitted and reflected by the grating, and can be calculated order by order,

$$\eta_{l\pm} \equiv \pm \frac{\overline{S}_{l\pm}^y}{S_i^y}, \quad (13)$$

with an obvious notation, and where the overbar represents the averages mentioned above. $S_{l\pm}^y = (1/8\pi)E_{l\pm}^z B_{l\pm}^{*y}$ for the TE case and an analogous expression for the TM case. The sum of all efficiencies adds up to one, due to energy conservation [33]. In our numerical calculations this property is used to verify the correctness of the results. For given values of the incident frequency and angle, we can know in advance how many real eigenmodes of the system and how many propagating diffraction orders exist (the rest being imaginary, see below). Thus, we truncate the matrix generated by Eq. (9) or (10) so as to obtain energy conservation up to ten significant digits.

In Fig. 2(a) we show an example of the transmitted diffraction efficiency as a function of frequency ω of the incident TE wave, for a slab of $d = 10K^{-1}$, $\epsilon_0 = 3$, $\epsilon_1 = 0.121$, and at an incident angle of $\theta = 28^\circ$; in the inset, the first resonance peak is shown at an enlarged scale. In Fig. 2(b) we show the TM case for the same parameters. The important feature we want to highlight is that, besides the expected wide undulations of the transmitted diffraction efficiency due to the finite thickness of the slab, there appear at irregular intervals very sharp peaks of large transmission or reflection. These are the guided-mode resonances that we explain in the next section.

III. GUIDED-MODE RESONANCES

A guided mode is a solution of Maxwell equations in all space, the absence of the incident wave ($E_0 = 0$ for TE and $B_0 = 0$ for TM), and in the form of propagating waves in the x direction. In the y direction we search for solutions propagating through the grating but evanescent outside it. These

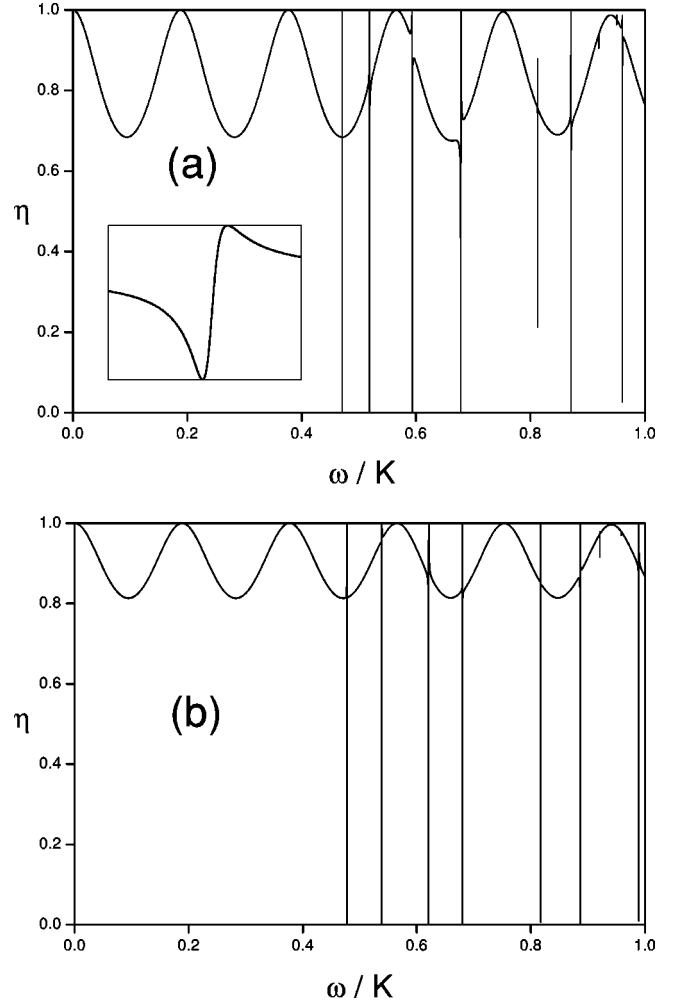


FIG. 2. Transmitted diffraction efficiency η as a function of frequency ω of the incident monochromatic wave, incident at an angle $\theta = 28^\circ$. The thickness of the diffraction grating is $d = 10K^{-1}$ with $\epsilon_0 = 3$ and $\epsilon_1 = 0.121$. (a) TE mode. In the inset, the first resonance is shown in the frequency interval from $\omega = 0.470751K^{-1}$ to $\omega = 0.470752K^{-1}$. (b) TM mode.

solutions are the analogs of guided modes in actual waveguides.

A. Dispersion relations

From the equations (9) and (10) we can find numerically the dispersion relation ω vs k_x by searching for the solutions mentioned above. We have performed such a procedure, as we show below, but first we want to sketch a simple analytical calculation of the dispersion relation that is valid in the limit $\epsilon_1 \ll \epsilon_0$. The reason for this approximation is that in this limit the modes inside the slab with different values of l are weakly coupled, see Eqs. (9) and (10). This way, for TE waves, we assume that we can set $\epsilon_1 \approx 0$ in Eq. (9), so that the eigenmodes are now approximately given by $a_{nl} \approx \delta_{nl}$ and the wave vectors κ_l by Eq. (12), i.e., the solution (11) has one term only. Therefore, we can search for propagating solutions inside the grating by considering only *one* mode at a time as if in a waveguide. Outside the grating we assume

the fields are evanescent and their y dependence is therefore given by $\exp(-|k_{ly}|y)$, where $|k_{ly}| = [(k_x + lK)^2 - \omega^2]^{1/2}$ [see Eq. (6)]. Clearly, k_x , ω , and K are such that κ_l and $|k_{ly}|$ are real. It is a simple exercise to show that these solutions exist if one of the following conditions are satisfied (cf. Refs. [2,3]):

$$\tan\left(\frac{1}{2}\kappa_l d\right) = \begin{cases} |k_{ly}|/\kappa_l & \text{TE} \\ -\kappa_l/|k_{ly}| & \text{TM} \end{cases} \quad (14)$$

$$\tan\left(\frac{1}{2}\kappa_l d\right) = \begin{cases} \epsilon_0|k_{ly}|/\kappa_l & \text{TM} \\ -\kappa_l/\epsilon_0|k_{ly}| & \text{TE} \end{cases} \quad (15)$$

For a given value of d , the above conditions are the dispersion relations ω vs k_x of the guided modes in the limit $\epsilon_1 \ll \epsilon_0$. In Fig. 3 we show the first Brillouin zone of the guided-mode dispersion relation ω vs k_x for different values of d for the TE case.

Figure 3(a) shows generic features of the dispersion relation for the TE case while Figs. 3(b) and 3(c) are particular examples for $d=1.0K^{-1}$ and $d=10.0K^{-1}$, respectively. In particular, in Fig. 3(b) we also show the dispersion relation obtained from the exact equations (9) for $\epsilon_1=0.121$ and $\epsilon_0=3.0$; the actual branches for these values are essentially identical to the approximate solutions (14), except at the Brillouin zone edges where the actual branches split; see the inset of Fig. 3(b).

The general features of the dispersion relation shown in Fig. 3(a) are the following. First, we can distinguish a region formed by the areas bounded from above by the solid lines defined by the change of the diffraction orders k_{ly} from real to imaginary [see Eq. (6)] and from below by the dashed lines defined by the first time an eigenmode $\kappa_n(K, \omega, k_x)$ becomes propagating [for small ϵ_1 this is approximately given by the change of the corresponding κ_n from imaginary to real, see Eq. (12)]. We find, both from the exact and the approximate calculations, that for any value of the thickness d of the grating all the guided-mode branches of the dispersion relation are contained within such a region; let us call it the “resonance region.” Of course, the location of the branches of the guided-mode dispersion relation depend explicitly on the given value of d , see Figs. 3(b) and 3(c). Second, from the numerical analysis of the structure of the eigenmodes of the *exact* equations (9) and (10), which are independent of d , one finds that below the lowest dashed line of the resonance region there are no propagating eigenmodes; between the first and the second dashed lines there is one; between the second and the third there are two, and so on. In a similar fashion, from the expression for k_{ly} , Eq. (6), one can see that below the lowest solid line there are no propagating diffraction orders outside the grating; between the first and second solid lines only the order $l=0$ propagates; between the second and the third, both the $l=0$ and the $l=-1$ orders propagate, and so on. Hence, we conclude that within the resonance region the number of *propagating* eigenmodes is always greater than the number of *propagating* diffraction orders. Outside the resonance region these numbers are equal and there are no guided modes. Since

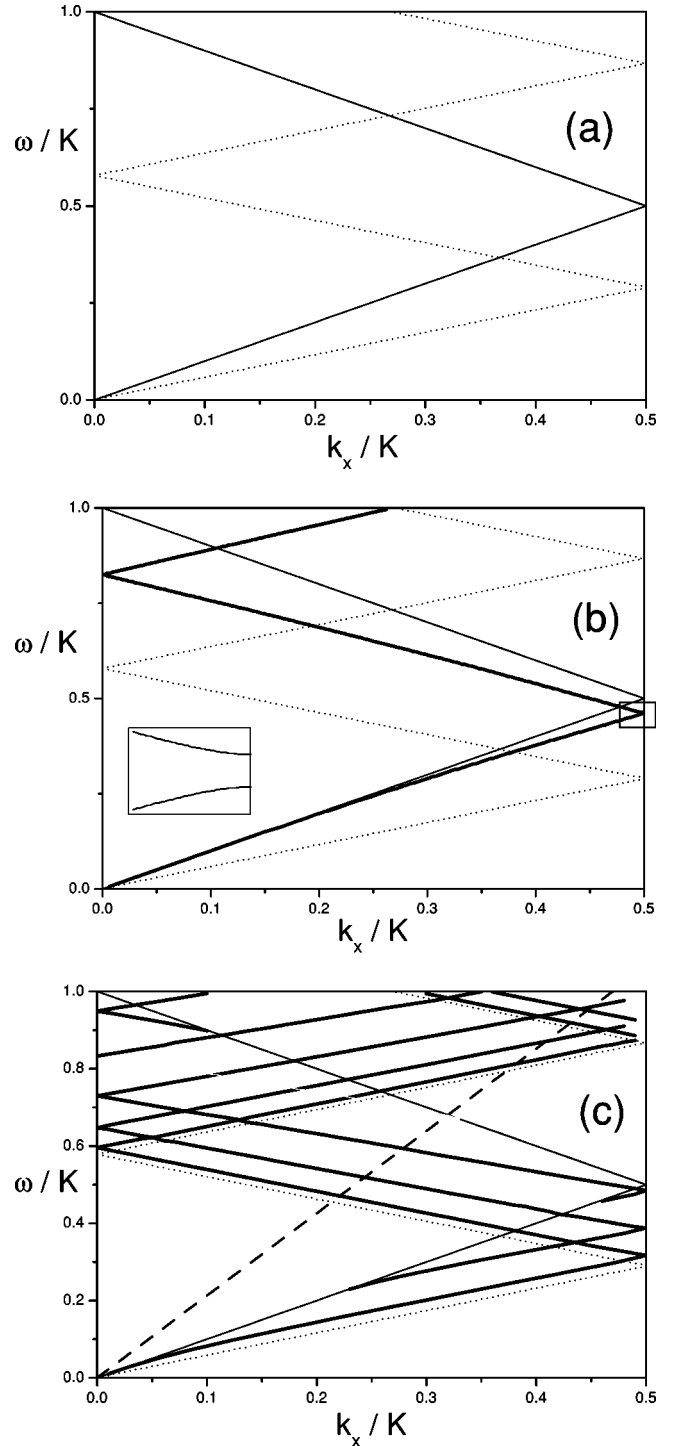


FIG. 3. (a) Generic features of the dispersion relation for s -polarized propagation, with $\epsilon_0=3$ and $\epsilon_1=0.121$. See text. (b) The thick solid line is the dispersion relation for a grating of thickness $d=1K^{-1}$. The inset shows the band gap at the Brillouin zone edge. (c) The thick solid lines is the dispersion relation for a grating of thickness $d=10K^{-1}$. The dotted line represents the incident wave vector at an angle of $\theta=28^\circ$.

each of the fields *outside* the grating couple to all the eigenmodes, this gives the known additional result that the guided modes cannot be strictly evanescent outside the grating since, in general, there are a finite number of propagating

diffraction orders. This in turn indicates that the branches of the dispersion relation in Figs. 3(b) and 3(c), have a *finite* width. In other words, the guided modes have a finite lifetime. On the other hand, it is this coupling that allows the guided modes to be excited. As an aside point we recall that the lines defined by $k_{ly}=0$ are the places where the so-called Wood anomalies [36] should appear. We have not found any peculiar behavior along these lines, other than being the place where the corresponding diffraction order emerges.

From the dispersion relation one can find the origin of the peaks of the diffraction efficiencies. Consider the case of the diffraction efficiency of the grating of thickness $d = 10.0K^{-1}$ for the TE mode shown in Fig. 2(a). In Fig. 3(c) we show the dispersion relation for this case together with a dashed line that represents the frequency of the incident wave, as a function of k_x , for an incident angle of $\theta=28^\circ$. The peaks of the corresponding diffraction efficiency [see Fig. 2(a)] appear at the frequencies where the dashed line crosses the dispersion relation of the guided modes. We point out that, by inspection of diffraction efficiencies for several different cases, one finds that as frequency is increased, the peaks of the guided-mode resonances tend to be diminished, and in some cases, they disappear altogether. We believe this is a consequence of the fact that as ω is increased, the number of propagating eigenmodes also increases, giving rise to a distribution of the incident energy among many modes, resulting in a poor excitation of the corresponding guided modes. We found that the resonances always are present when the incident wave vector is of the order of the grating wave vector.

B. Physical origin of the resonances

The fact that inside the resonance region the number of *propagating* eigenmodes is larger than the number of *propagating* diffraction orders suggests a simple physical explanation for the resonance phenomenon. For this, we refer to Fig. 4 where we show the transmitted diffraction efficiency as a function of the *thickness* d of the diffraction slab, and for a fixed value of the incident wave vector k_x and frequency ω , for the TE case. An experiment of this sort would certainly be difficult to perform but it can be theoretically analyzed. The values of k_x and ω were chosen within the resonance region where there are two propagating modes inside, κ_0 and κ_1 , and only one diffraction order ($l=0$) outside the grating. The mode κ_0 and the order $l=0$ are very strongly coupled giving rise to the smooth oscillations of the transmission efficiency. The mode κ_1 is mostly coupled to the evanescent order $l=-1$. However, due to finite size of ϵ_1 all the modes are coupled. Notice that the resonance peaks in Fig. 4 appear *periodically*. As we show below, the resonances are found to be separated by $\Delta d = \pi/\kappa_1$. The separation of the resonances may be expected but what is not so obvious is the position of the first resonance. Since $\epsilon_1 \ll \epsilon_0$ we can proceed in a perturbationlike fashion. To the very lowest order, one can consider that the propagating diffraction order $l=0$ couples only to the propagating mode κ_0 and as said above, the result of this analysis fits very well the smooth oscillations of the efficiencies but shows no resonance peaks. To the next order,

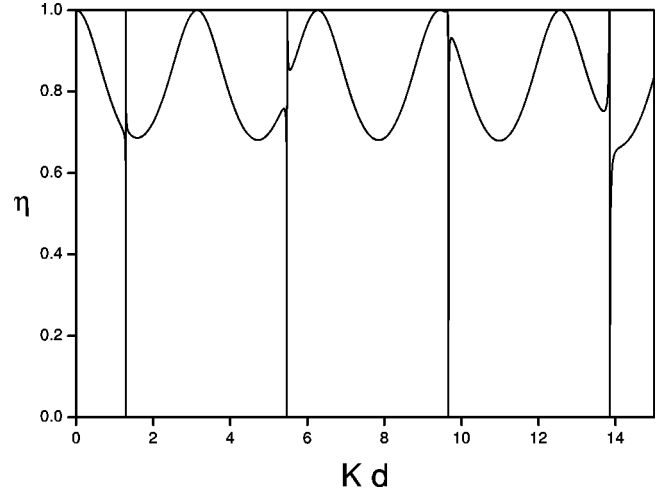


FIG. 4. Transmitted diffraction efficiency η as a function of grating thickness d for incident s -polarized light at a frequency $\omega = 0.6K^{-1}$ and at an angle $\theta=28^\circ$. $\epsilon_0=3$ and $\epsilon_1=0.121$. For these parameters there are two propagating modes within the slab and one propagating diffraction order outside of it. The resonances appear periodically due to the condition $\epsilon_1 \ll \epsilon_0$.

the effect of the coupling between the modes within the grating gives rise to the other propagating mode, κ_1 . Consider now the propagation of a front of the latter mode starting at an arbitrary position x in one of the inside walls of the grating. When it reaches and bounces off the opposite wall, it acquires a phase $2\kappa_1 - 2\phi$. When it returns to the original wall, it acquires an additional phase -2ϕ . Thus, the total phase difference between these two fronts is $2\kappa_1 - 4\phi$. When this phase equals $2m\pi$ the fields add up in phase yielding the resonance. That is,

$$\kappa_1 d - 2\phi = m\pi. \quad (16)$$

The phase ϕ can easily be calculated by assuming that this mode only couples to the evanescent order $l=-1$ outside the grating. One finds,

$$\tan \phi = \frac{|k_{-1y}|}{\kappa_1}. \quad (17)$$

For even values of m the equations (16) and (17) can be combined and the result can be cast as the positive solution of Eq. (14) for $l=-1$. An analogous procedure for the odd values of m yields the corresponding negative solution. We can repeat the analysis for each new excited mode κ_n , assuming that it couples only to the corresponding l th evanescent order; the result is the same as that given by the equations above. Thus, the resonance conditions given by the generalization of Eqs. (16) and (17) for all l , are equivalent to the guided-mode dispersion relation given by Eq. (14). An analogous description exists for the TM case.

C. Dependence on ϵ_1

The positions of the resonances in the diffraction efficiencies, which were calculated with the exact equations, are

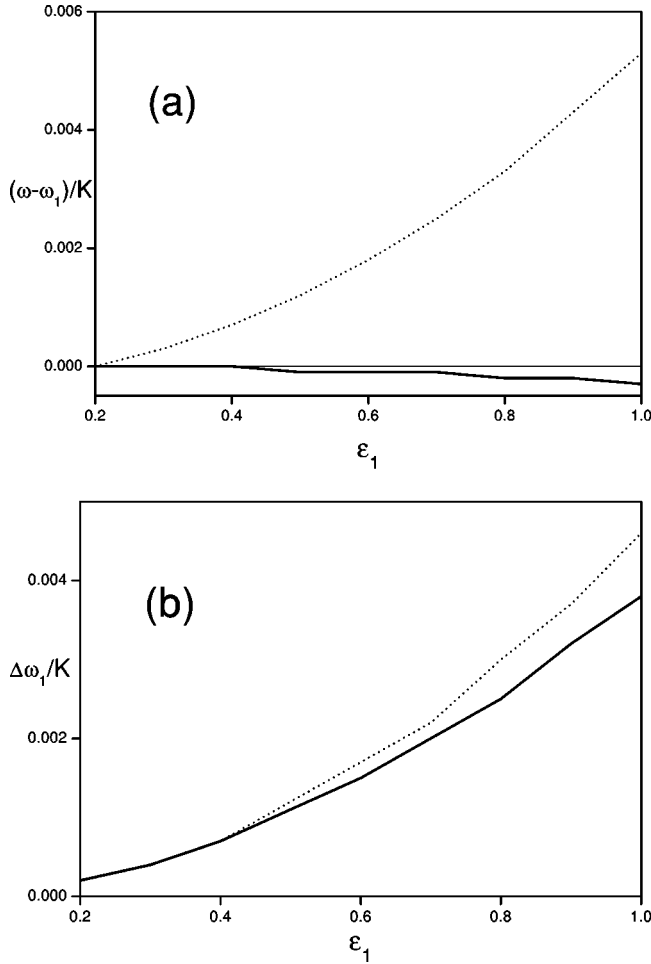


FIG. 5. (a) Shift $(\omega - \omega_1)$ of the first resonance for a grating of thickness $d = 1K^{-1}$ (solid line) and $d = 5K^{-1}$ (dotted line) as a function of ϵ_1 . (b) Width $\Delta\omega_1$ of the same resonance for the same set of parameters.

very accurately described by the approximate dispersion relations (14) and (15) that neglect the finiteness of the grating modulation ϵ_1 . This is a consequence of the fact that the values $\epsilon_1 = 0.121$ and $\epsilon_0 = 3.0$ agree very well with the requirement $\epsilon_1 \ll \epsilon_0$. But, the coupling between different modes inside the grating makes the guided modes, as called in the literature, “leaky.” In other words the grating guided modes have a finite lifetime. Obviously, the lifetime is longer the smaller ϵ_1 is, compared with ϵ_0 . Besides becoming wider as ϵ_1 is increased, the positions of the resonances are shifted from their predicted value at $\epsilon_1 = 0$. In Fig. 5(a) we show the shift $(\omega - \omega_1)$ of the position of the first resonance for $d = 1.0K^{-1}$ and for $d = 5.0K^{-1}$ as a function of ϵ_1 ; in the former case, the resonance is centered at $\omega_1 \approx 0.62K^{-1}$ for $\epsilon_1 = 0$ and at $\omega_1 \approx 0.5K^{-1}$ in the latter case. In Fig. 5(b) we show the width $\Delta\omega_1$ of the same resonances as a function of ϵ_1 . These figures exemplify the generic behavior that the peaks become wider as ϵ_1 is increased and that their positions shift in frequency, though the direction of the shift may be positive or negative. We find that these effects are more prominent for larger values of d .

Clearly, if ϵ_1 becomes of the order of ϵ_0 the resonance “lines” are so wide that the concept of “guided mode” may no longer be meaningful. However, we point out that no matter how large ϵ_1 is, i.e., even larger than ϵ_0 , solutions to the Maxwell equations exist [that is, of Eqs. (9) and (10)] with the expected result that the different propagating diffraction orders are more intense than for smaller values of ϵ_1 . We find it interesting that even though the dielectric function $\epsilon(x)$ becomes negative in some *spatial* regions, energy is still conserved. That is, the diffraction efficiencies add up to one. It is not very clear how one could prepare a diffraction grating with these characteristics.

IV. BRAGG PEAKS

Due to the periodicity of the dielectric grating in the x direction, it is expected that there exist peaks in the diffraction efficiencies at incident angles given by the Bragg condition,

$$2k \sin \theta = nK, \quad (18)$$

with n a positive integer. Indeed, it is known that these peaks appear in the transmitted fields of the first diffraction order ($l = -1$ in our notation) at the Bragg angle with $n = 1$, for “thick” diffraction gratings. There have been several approximate analysis of these peaks (both from the coupled-wave theory and from the treatment of light diffracted by ultrasonic waves) [5–7], but they are valid only in a reduced range of parameters. Here, we report this case as well as higher order Bragg peaks, i.e., $n > 1$.

From the dispersion relation, or from Eq. (6) for k_{ly} , the y component of the l th diffraction order, we know how many diffraction orders propagate at a given incident frequency and angle of incidence. For instance, for $0 \leq \omega \leq K$ there are at most two diffraction orders, $l = 0$ and $l = -1$. As the frequency is increased there appear higher orders, and they do so in pairs, $l = m - 1$ and $l = -m$ with m a positive integer. The main result we want to report here is that, in general, the diffraction orders $l = -m$ show peaks at angles given by $n = m$ in the Bragg condition (18). Although the following is not a rigorous analysis, it appears that at the different Bragg angles (i.e., at the different values of n) the corresponding diffraction order, $l = -m$, is diffracted in the same direction as the $l = 0$ transmitted order. This can be seen from the expression for the y component of the diffracted wave vector, which can be rewritten as

$$k_{ly} = [\omega^2 - (2\omega \sin \theta + lK - k_x)^2]^{1/2}, \quad (19)$$

where we have used the fact that $k_x = \omega \sin \theta$. When the angle of incidence obeys the Bragg condition for $n = -l$, Eq. (18), we see that propagation of the $l = -n$ order, $k_{ly} = k_y = \omega \cos \theta$, is in the direction of the incident wave. Thus, the transmission efficiency is enhanced. For positive values of l the above expression cannot be satisfied at any angle (smaller than 90°). To the best of our knowledge the correlation between higher diffraction orders and higher order Bragg peaks has not been reported before.

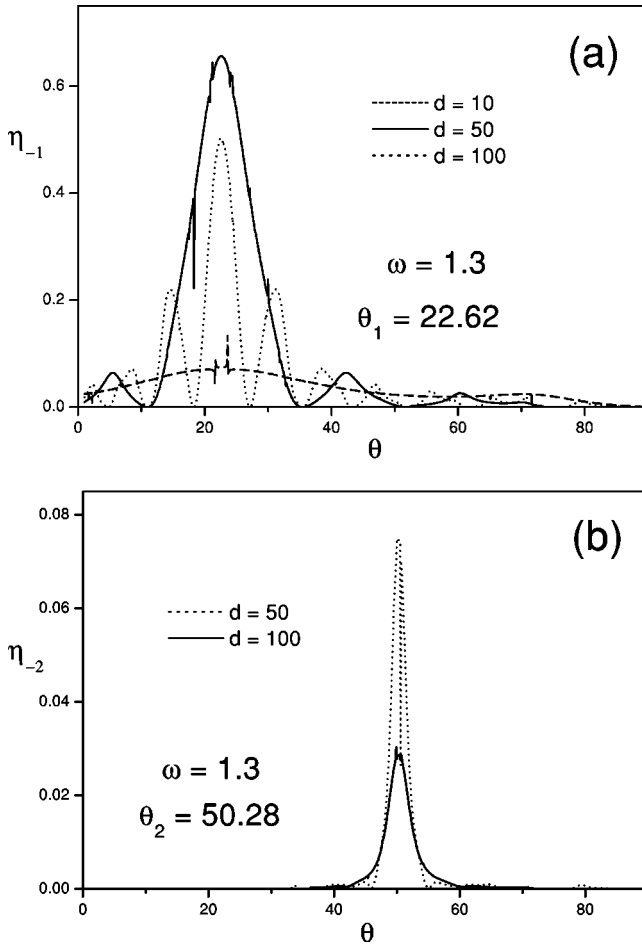


FIG. 6. Transmitted diffraction efficiency η as a function of the angle of incidence θ (deg) for a frequency $\omega = 1.3K^{-1}$, for different grating thickness. (a) $l = -1$ diffraction order; the maximum appears at the Bragg angle with $n = 1$, Eq. (18). (b) $l = -2$ diffraction order; the maximum appears at the Bragg angle with $n = 2$, Eq. (18).

Figures 6 and 7 show examples of this behavior for different thickness d of the diffraction gratings. We highlight two features of these figures. First, one finds that the peaks are more pronounced as d is increased, however, this behavior is not monotonic. For instance, one sees from Fig. 6 that for the order $l = -1$ at the Bragg angle $n = 1$, the peak is greater for $d = 50K^{-1}$ than for $d = 100K^{-1}$, while from Fig. 7 we find that the opposite is true for $l = -2$ at the Bragg angle $n = 2$. Second, besides the main peaks there exist secondary peaks that appear to be Fabry-Perot-like interferences due to the finite size of the grating. These secondary peaks (especially for $d = 100K^{-1}$) may become even greater than the Bragg peak and in some cases this peak is completely masked by the secondary ones [see Fig. 7(a)]. The diffraction orders with $l > 0$ do not show any appreciable peak at any Bragg angle. Their behavior appears to be dominated mainly by the Fabry-Perot-like interferences.

We would like to point out that from equation (18) that the higher order Bragg peaks can also be understood in a different way. That is, as if they are the Bragg peaks of the overtones of the grating wave vector K , i.e., of nK . This

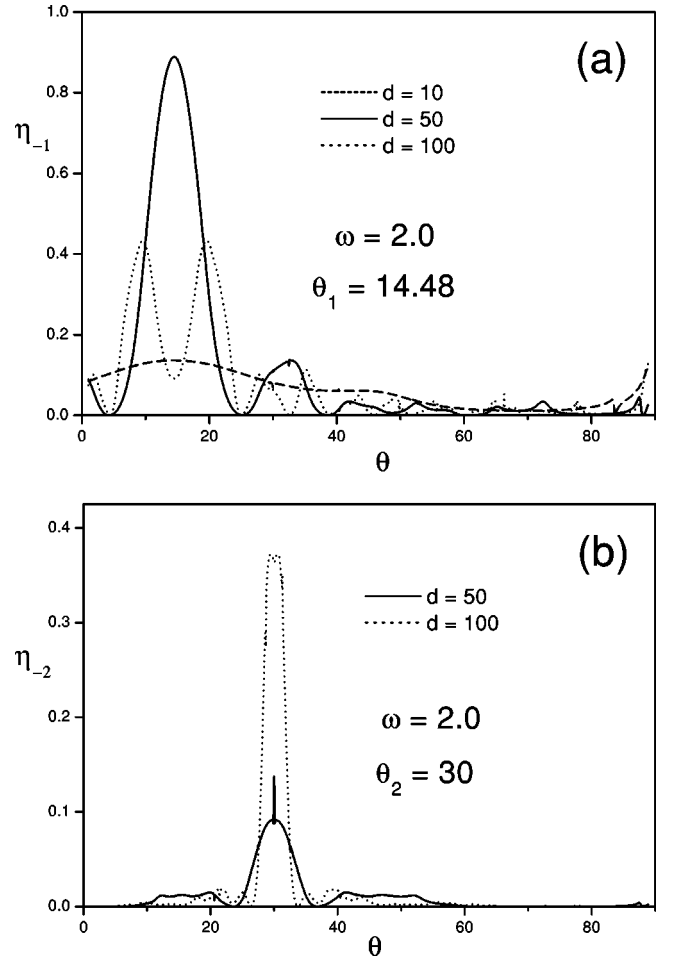


FIG. 7. Transmitted diffraction efficiency η as a function of the angle of incidence θ (deg) for a frequency $\omega = 2.0K^{-1}$, for different grating thickness. (a) $l = -1$ diffraction order; the maximum appears at the Bragg angle with $n = 1$, Eq. (18). (b) $l = -2$ diffraction order; the maximum appears at the Bragg angle with $n = 2$, Eq. (18).

interpretation may be relevant to the experiments performed by Nelson and coworkers [28,29], in spatiotemporal gratings created in ferroelectric crystals by two crossed ultrashort laser pulses. They find responses of diffracted pulses not only at the Bragg angle of the grating wave vector but at its overtones as well. Their interpretation is that the grating also has those wave vector components due to nonlinear excitations in the crystal. It may be relevant to include in such an analysis the possibility that a grating with only one wave vector component can give rise to responses at its overtones as well.

V. CONCLUSIONS AND FINAL REMARKS

We have presented and analyzed the dispersion relation of the guided-mode resonances that appear in sinusoidally modulated dielectric diffraction gratings. The approximate theory, based on assuming only one propagating eigenmode inside the grating and one evanescent wave outside of it, gives a very accurate description of the dispersion relation in the limit in which the modulation ϵ_1 is much smaller than the

background mean dielectric constant ϵ_0 . As expected, the number of branches of the dispersion relation increases as the thickness d of the grating is increased. The gaps of the branches at the band edges of the first Brillouin zone can only be described through the exact theory. The dispersion relation allows for an overall understanding of the behavior of the diffraction efficiencies, for the different orders, as a function of frequency and angle of incidence. We have found that a necessary condition for the resonances to appear is that the number of propagating material eigenmodes must be larger than the number of propagating diffraction orders. This indicates the physical origin of the resonances: first, those extra modes are excited through the coupling with the diffracted orders, and when the inside multiple reflections are in phase, the resonance occurs. In the regions where the number of propagating modes inside the grating are equal to the propagating diffraction orders outside of it, there are no resonances. Although the dispersion relation predicts the location of the resonances, we found that these are more clearly seen for values of the incident frequency of the order of the wave vector grating (divided by c). For higher values of the frequency, the amplitudes of the resonances tend to be diminished and in some cases completely suppressed. As the modulation ϵ_1 is increased relative to ϵ_0 , the coupling among the modes is also increased, giving rise to shifts in the positions of the resonances as well as a reduction in their lifetimes. We found that this behavior depends strongly on the thickness d of the grating; for instance, for $d = 10.0K^{-1}$, the lowest resonance is so shifted that for $\epsilon_1 \approx 1$ it completely

disappears. We were not able to find an analytical description for the shifts and the widening of the resonances. We emphasize that, in principle, any question regarding these systems can be answered through the exact coupled-wave theory [33]; with the current available computer capabilities one can achieve the necessary numerical accuracy.

Finally, it is very interesting and relevant to point out the result that the locations of the Bragg peaks at different orders are correlated with the different propagating diffraction orders. We showed that this correlation occurs at the angle where the corresponding diffraction orders propagate in the same direction as the incident wave. In the several approximate theories that deal with the Bragg diffraction [5–7], only the first Bragg peak is analyzed and it is found that this effect is more pronounced for “thicker” gratings (say, $d > 10K^{-1}$). We have found that, although the effect is better seen for thicker gratings, the behavior is not monotonic and, depending on the incident frequency and the thickness d of the grating, the background Fabry-Perot-like interference peaks may be of the order of, or even larger than the Bragg peak itself. The full understanding of this complicated behavior deserves further theoretical analysis.

ACKNOWLEDGMENTS

This work was supported by CONACyT (Mexico) through Grant No. 32634-E. S.N.-H. acknowledges support from DGEP, UNAM, Mexico.

-
- [1] A. Hessel and A.A. Oliner, *Appl. Opt.* **4**, 1275 (1965).
 [2] S.S. Wang, R. Magnusson, J.S. Bagby, and M.G. Moharan, *J. Opt. Soc. Am. A* **7**, 1470 (1990).
 [3] S.S. Wang and R. Magnusson, *Appl. Opt.* **32**, 2606 (1993).
 [4] T. Peter, R. Bräuer, and O. Bryngdahl, *Opt. Commun.* **139**, 177 (1997).
 [5] C.B. Burckhardt, *J. Opt. Soc. Am. A* **56**, 1502 (1966).
 [6] M.G. Moharam, T.K. Gaylord, and R. Magnusson, *J. Opt. Soc. Am.* **70**, 300 (1980).
 [7] M.G. Moharam, T.K. Gaylord, and R. Magnusson, *Opt. Commun.* **32**, 14 (1980).
 [8] F. Schreier, M. Schmitz, and O. Bryngdahl, *Opt. Lett.* **23**, 576 (1998).
 [9] F. Schreier, M. Schmitz, and O. Bryngdahl, *Opt. Lett.* **23**, 1337 (1998).
 [10] F. Schreier and O. Bryngdahl, *J. Opt. Soc. Am. A* **17**, 68 (2000).
 [11] E.N. Glytsis and T.K. Gaylord, *Appl. Opt.* **28**, 2401 (1989).
 [12] J.C.W.A. Costa and A.J. Giarola, *IEEE Trans. Antennas Propag.* **43**, 529 (1995).
 [13] D. Rosenblatt, A. Sharon, and A.A. Friesem, *IEEE J. Quantum Electron.* **33**, 2038 (1997).
 [14] T. Tamir and S. Zhang, *J. Opt. Soc. Am. A* **14**, 1607 (1997).
 [15] G. Levy-Yurista and A.A. Friesem, *Appl. Phys. Lett.* **77**, 1596 (2000).
 [16] S.S. Wang and R. Magnusson, *Opt. Lett.* **19**, 919 (1994).
 [17] J. Saarinen, E. Noponen, and J. Turunen, *Opt. Eng.* **34**, 2560 (1995).
 [18] P. Rochon, A. Natansohn, C.L. Callender, and L. Robitaille, *Appl. Phys. Lett.* **71**, 1008 (1997).
 [19] S.M. Norton, T. Erdogan, and G.M. Morris, *J. Opt. Soc. Am. A* **14**, 629 (1997).
 [20] D. Shin, S. Tibuleac, T.A. Maldonado, and R. Magnusson, *Opt. Eng.* **37**, 2634 (1998).
 [21] R. Magnusson, D. Shin, and Z.S. Liu, *Opt. Lett.* **23**, 612 (1998).
 [22] D.L. Brundrett, E.N. Glytsis, and T.K. Gaylord, *Opt. Lett.* **23**, 700 (1998).
 [23] Z.S. Liu, S. Tibuleac, D. Shin, P.P. Young, and R. Magnusson, *Opt. Lett.* **23**, 1556 (1998).
 [24] F. Lemarchand, A. Sentenac, E. Cambriil, and H. Giovannini, *J. Opt. A, Pure Appl. Opt.* **1**, 545 (1999).
 [25] R.J. Stockermans and P.L. Rochon, *Appl. Opt.* **38**, 3714 (1999).
 [26] R.R. Boye and R.K. Kostuk, *Appl. Opt.* **39**, 3649 (2000).
 [27] Z. Hegedus and R. Netterfield, *Appl. Opt.* **39**, 1469 (2000).
 [28] C.J. Brennan and K.A. Nelson, *J. Chem. Phys.* **107**, 9691 (1997).
 [29] K.A. Nelson and coworkers, *J. Chem. Phys.* **114**, 1443 (2001).
 [30] M.G. Moharam and T.K. Gaylord, *J. Opt. Soc. Am.* **71**, 811 (1981).
 [31] M.G. Moharam and T.K. Gaylord, *J. Opt. Soc. Am.* **73**, 451 (1983).

- [32] M.G. Moharam and T.K. Gaylord, J. Opt. Soc. Am. **73**, 1105 (1983).
- [33] T.K. Gaylord and M.G. Moharam, Proc. IEEE **73**, 894 (1985). This is a very comprehensive review of this theory as well as comparisons with other approximated schemes.
- [34] M. Born and E. Wolf, *Principles of Optics: Electromagnetic Theory of Propagation, Interference and Diffraction of Light*, 1st ed. (Editorial, Country, 1959).
- [35] The technique proposed by Moharam and Gaylord, Refs. [30–33], to solve the eigenvalue problem of the fields inside the gratings does not lead to an orthogonal matrix and, therefore, the property that the corresponding eigenvalues must be real does not hold.
- [36] R.W. Wood, Philos. Mag. **4**, 396 (1902).